

# Potential mechanisms of osteoprotegerin-induced damage to osteoclast adhesion structures via P2X7R-mediated MAPK signaling

YONGGANG MA<sup>1-3\*</sup>, XUENI SHI<sup>1-3\*</sup>, HONGYAN ZHAO<sup>1-3</sup>, RUILONG SONG<sup>1-3</sup>,  
HUI ZOU<sup>1-3</sup>, JIAQIAO ZHU<sup>1-3</sup> and ZONGPING LIU<sup>1-3</sup>

<sup>1</sup>College of Veterinary Medicine, Yangzhou University; <sup>2</sup>Jiangsu Co-innovation Center for Prevention and Control of Important Animal Infectious Diseases and Zoonoses; <sup>3</sup>Joint International Research Laboratory of Agriculture and Agri-Product Safety of The Ministry of Education of China, Yangzhou University, Yangzhou, Jiangsu 225009, P.R. China

Received September 29, 2021; Accepted January 18, 2022

DOI: 10.3892/ijmm.2022.5115

**Abstract.** Osteoprotegerin (OPG) is a negative regulator of osteoclast formation by competing with receptor activator of the nuclear factor- $\kappa$ B (NF- $\kappa$ B) ligand (RANKL) for RANK. OPG is not only a soluble decoy receptor for RANKL, but is also considered as a direct effector of osteoclast functions. However, the mechanisms responsible for OPG-induced changes to osteoclast bone resorption functions remain unknown. P2X7R is involved in the process of multi-nucleation and cell fusion. Therefore, in the present study, mitogen-activated protein kinase (MAPK) inhibitors and the RNA interference of purinergic receptor P2X7 (P2X7R) were used to examine the effects of P2X7R-mediated MAPK signaling on changes to osteoclast adhesion structure induced by OPG; for this purpose, western blot analysis and immunofluorescence staining were performed. The results revealed that OPG inhibited osteoclast adhesion-related protein expression, disrupted adhesion protein distribution, and destroyed osteoclast filopodia and lamellipodia structures. The inhibitors partially restored osteoclast adhesion structure, including

protein expression, distribution and cell morphology. The absence of P2X7R markedly inhibited osteoclast formation, and subsequent OPG treatment accelerated the damage to adhesion structures. However, P2X7R activation significantly recovered the phosphorylation of paxillin, vinculin, phosphorylated protein tyrosine kinase 2 and SRC proto-oncogene, non-receptor tyrosine kinase induced by OPG, and their distribution was uniform at the osteoclast periphery. P2X7R silencing suppressed the phosphorylation of MAPK. On the whole, the findings of the present study highlight a key role of P2X7R/MAPK signaling in osteoclast adhesion, and provide a novel therapeutic target for bone disease.

## Introduction

Osteoclasts are multinucleated bone-resorbing cells that differentiate from macrophages in bone marrow. Osteoclastogenesis is primarily governed by two key cytokines, receptor activator of the nuclear factor- $\kappa$ B (NF- $\kappa$ B) ligand (RANKL) and macrophage colony-stimulating factor (M-CSF) (1). Osteoprotegerin (OPG), a glycoprotein mainly synthesized by osteoblasts, functions as a decoy receptor for RANKL. OPG binds to RANK and blocks its activity, which results in the inhibition of osteoclast differentiation and subsequent bone resorption (2). RANK, RANKL and the OPG system can form a tertiary complex, suggesting that OPG is not only a soluble decoy receptor for RANKL, but can also be considered as a direct effector of osteoclast functions (3).

OPG disrupts the attachment structure of osteoclasts and activates SRC proto-oncogene, non-receptor tyrosine kinase (SRC) (4). SRC is an adaptor protein that competes for the reduced amount of phosphorylated protein tyrosine kinase 2 (PYK2) remaining following OPG short-term treatment via calcium- and extracellular signal-regulated kinase (ERK)-dependent signaling pathways (5). In this process, OPG short-term treatment reduces the intracellular calcium concentration. However, adenosine triphosphate (ATP) can increase the calcium concentration and inhibit damage to adhesion structures induced by OPG (6). Extracellular ATP is viewed as a primary messenger as it stimulates purinergic receptor

*Correspondence to:* Dr Jiaqiao Zhu or Dr Zongping Liu, College of Veterinary Medicine, Yangzhou University, 88 South University Avenue, Yangzhou, Jiangsu 225009, P.R. China  
E-mail: jqzhu1998@163.com  
E-mail: liuzongping@yzu.edu.cn

\*Contributed equally

**Abbreviations:** OPG, osteoprotegerin; RANKL, receptor activator of the nuclear factor- $\kappa$ B (NF- $\kappa$ B) ligand; M-CSF, macrophage colony-stimulating factor; P2X7R, purinergic receptor P2X7; PYK2, phosphorylated protein tyrosine kinase 2; ERK, extracellular signal-regulated kinase; JNK, c-Jun N-terminal kinase; NFATc1, nuclear translocation of nuclear factor of activated T-cells 1

**Key words:** osteoclast, P2X7R, podosome, ERK/p38/JNK, osteoprotegerin

P2X7 (P2X7R) at the cell surface of autocrine or paracrine cells. Additionally, P2X7R has been detected in osteoclasts and osteoblasts. Therefore, P2X7R may play an important role in osteoclast function.

P2X receptors are ATP-gated, non-selective cation channels, which are divided into seven subtypes. When ATP binds to a P2X receptor, it causes cytomembrane depolarization and the subsequent elevation of the intracellular calcium concentration, either by direct  $\text{Ca}^{2+}$  permeation or by the activation of voltage-gated  $\text{Ca}^{2+}$  channels, which triggers a range of signaling cascades, resulting in both short- and long-term cellular events (7). P2X receptors are widely expressed in a number of tissues and cells (8). However, P2X7R differs from the other P2XRs to a certain degree. First, the brief activation of P2X7R results in rapid membrane depolarization similar with other P2XR; however, within seconds, a more profound development of an additional permeability state occurs, which allows for the permeation of large cations with a molecular weight of up to 900 kDa. Secondly, 3'-O-(4-Benzoyl)benzoyl ATP (BzATP) is a more potent activator of P2X7R than ATP, and its activation induces cellular fusion or apoptosis (9). However, a recent study indicated that purinergic signaling occurs in bone metabolism (10); therefore, the present study focused on P2X7R-mediated signaling in bone.

P2X7R plays an important role in bone metabolism, being expressed by both osteoclasts and osteoblasts, in which it plays a role in modulating differentiation, function and lifespan (11). It has also been demonstrated that BALB/c *P2x7r<sup>-/-</sup>* mice exhibit increased bone loss; BALB/c *P2x7r<sup>-/-</sup>* derived precursors have been shown to generate a slightly greater number of osteoclasts, although with a significant reduction in the amount of resorption per osteoclast (12). The nuclear translocation of nuclear factor of activated T-cells 1 (NFATc1) in RANKL- and M-CSF-primed monocytes and in mature, resorbing osteoclasts has been shown to be dependent on P2X7R activation (13). Moreover, abolishing P2X7R activity would interfere with calcium signaling, thereby influencing osteoclast function by affecting the formation of the ruffled border and subsequently, bone resorption (14). Therefore, P2X7R plays a critical role in the regulation of osteoclast fusion and resorption. However, it is not clear whether P2X7R participates in regulating osteoclast adhesion structure function induced by OPG.

The present study aimed to examine the regulatory effects of P2X7R on damage to osteoclast adhesion structures induced by OPG. It was hypothesized that the effects of P2X7R on OPG-induced damage to osteoclast function would be mediated via mitogen-activated protein kinase (MAPK) signaling. Moreover, P2X7R may be a novel target with OPG in the treatment of osteoporosis.

## Materials and methods

**Animals.** In the present study, all mice were provided by Yangzhou University. BALB/c male mice were used (weight, 10–15 g; age, 4 weeks). All mice were sacrificed by cervical dislocation method and mouse death was verified by the cessation of respiratory movements. A total of 40 mice were used for the isolation of primary cells. No mouse died during the experimental period, which was 4 weeks. Mouse health and behavior were monitored every day. All mice were kept in

specific pathogen-free (SPF) animal housing with a temperature of 18–25°C, a humidity of 30–50% and a 12-h dark/light cycle every day for 1 month. All mice were also provided with free access to food and water.

**Cell culture and osteoclast induction.** Mouse bone marrow-derived macrophages (BMMs) were used for osteoclast differentiation. BMMs can continually proliferate under M-CSF stimulation, and can differentiate into multinuclear cells under RANKL stimulation (4). In the present study, BMMs were isolated from the femurs and tibiae of BALB/c mice, the marrow was aspirated from the marrow cavity using a syringe to collect the cells, seeded and cultured in  $\alpha$ -minimal essential medium (MEM) (Gibco; Thermo Fisher Scientific, Inc.) with 10% fetal bovine serum (FBS) (Gibco; Thermo Fisher Scientific, Inc.) overnight in humidified atmosphere of 5%  $\text{CO}_2$  at 37°C. The experimental procedures were approved by the Ethics Committee of Yangzhou University [SYXK (Su) 2017-0044]. The suspended cells were used as osteoclast precursors and further cultured in the presence of M-CSF (30 ng/ml) and RANKL (60 ng/ml; R&D Systems, Inc.) for 5 days. The medium was changed every 2 days. At the end of the culture period, mature osteoclasts were visualized using tartrate-resistant acidic phosphatase (TRAP) staining as described below. The expression of osteoclast adhesion proteins was examined by using various concentrations of OPG (0, 20, 40 and 80 ng/ml); according to the results, the concentration of 80 ng/ml OPG was used in follow-up experiments.

**Cell transfection.** A P2X7R short hairpin RNA (shRNA) knockdown construct was constructed by Hanheng (Shanghai) Corporation Ltd. Transfection was performed using shRNA-P2X7R and NC-shRNA adenovirus and the silencing efficiency was determined using western blot analysis. The cell transfection method was previously described in the study by Ma *et al.* (14). An adenoviral vector containing shRNA-P2X7 (MOI, 1–3) was introduced into BMMs in the presence of M-CSF (30 ng/ml); after 24 h, the transduction efficiency was observed using fluorescence microscopy, and the silencing and overexpression efficiency were determined using western blot analysis. NC-shRNA was used as the non-targeting sequence, and the sequences of the shRNAs and NC-shRNA were as follows: NC-shRNA: Top strand, aattcGTTCTCCGAACGTGTCACGTAATTCAAGAGATTACGACACGTTTCGCAGATTGTTTg; bottom strand, gatccAAAAAATTCTCCGAACGTGTCACGTAATCTCTTGAATTACGTGACACGTTTCGGAGAACg. shRNA: Top strand, AATTCGACGAAGTTAGGACACAGCATCTTTGttcaagagaCAAAGATGCTGTGTCTTAACCTTCGTTttttt; bottom strand, GATCCAAAAAACAAGTTAGGACACAGCATCTTTGTctcttgaaCAAAGATGCTGTGTCCTAACCTTCGTCg.

**TRAP staining.** BMMs were cultured in the presence of RANKL and M-CSF, following BMMs were treated with A438079 (ab120413; Abcam) for 12 h, after 5 days, the cells were fixed in 10% paraformaldehyde for 10 min. After washing with PBS, the cells were stained using a TRAP-Kit 387A (Sigma-Aldrich; MerckKGaA) according to the manufacturer's instructions. TRAP-positive mature osteoclasts having

more than three nuclei were observed and counted using a light microscope (LEICA DMI 3000B; Leica Microsystems GmbH).

**Western blot analysis.** The cells were washed twice with cold PBS and lysed in radioimmunoprecipitation assay (RIPA) buffer (Beyotime Institute of Biotechnology) on ice for 30 min, and then centrifuged at 12,000 x g for 10 min to precipitate the cell debris at 4°C. The protein concentration was determined using a bicinchoninic acid (BCA) protein assay kit. The western blot analysis protocol was as previously described in the study by Fathi *et al* (15). Equal amounts of protein were separated using 10-12% SDS-PAGE. The proteins in the gel were transferred onto polyvinylidene fluoride (PVDF) membranes. After blocking with 5% skim milk in Tris-buffered saline-Tween-20 (TBST) for 2 h at room temperature, the membranes were incubated overnight with primary antibodies at 4°C. The primary antibodies were as follows: Anti-phospho (p)-PYK2 (phospho Y402) (1:1,000; ab4800), anti-PYK2 (1:1,000; ab32571), anti-vinculin (1:1,000; ab129002) (all from Abcam), anti-p-vinculin (1:1,000; SAB4301470; Sigma-Aldrich; Merck KGaA), anti-paxillin (1:1,000; ab32084), anti-p-paxillin (phospho Y31; 1:1,000; ab4832), anti-p-paxillin (phospho S126; 1:1,000; ab24402), anti-integrin  $\alpha$ v (1:1,000; ab179475), P2X7 (1:1,000; ab259942) (all from Abcam), anti-integrin  $\beta$ 3 (1:500; ET1606-49; HUABIO), anti-SRC (1:1,000; #2109), anti-p-SRC (Tyr416; 1:1,000; #2101) and anti-p-SRC (Tyr527; 1:1,000; #2105), ERK (1:1,000; #4695), p-ERK (1:1,000; #4370), JNK (1:1,000; #9252), p-JNK (1:1,000; #4668), p38 (1:1,000; #8690), p-p38 (1:1,000; #4511), (all from Cell Signaling Technology, Inc.). The following day, the membranes were washed and incubated with horseradish peroxidase (HRP)-conjugated secondary antibodies (1:5,000; #7076 and #7074; Cell Signaling Technology, Inc.) for 2 h at room temperature. The immunoreactive proteins on the membranes were then visualized using chemiluminescence (cat. no. P2300, New Cell & Molecular Biotech). Densitometric quantification was performed using ImageJ software 1.48 (National Institutes of Health). The protein expression level was calculated according to the gray value of the bands.

**Immunofluorescence staining.** The cells were cultured for 5 days following treatment with various reagents [U0126 (ERK inhibitor), 5  $\mu$ M; SP600125 (JNK inhibitor), 10  $\mu$ M; SB202190 (MAPK inhibitor), 5  $\mu$ M; MedChemExpress] and 30  $\mu$ M BzATP (ab120444; Abcam) for 30 min and OPG (80 ng/ml) for 12 h, and then fixed using 10% paraformaldehyde for 30 min, permeabilized with 0.3% Triton X-100 for 20 min, and washed with PBS three times. The cells were first incubated in 5% skim milk in TBST for 30 min, and then incubated overnight with primary antibodies at 4°C, (the primary antibodies were the same as those used for western blot analysis; dilution, 1:200), washed three times in PBS. Subsequently, the coverslips were washed and incubated for 2 h at room temperature with Alexa Fluor® 488-conjugated secondary antibody (cat. no. A0428; 1:200). F-actin was stained with phalloidin (ab176756; Abcam) for 40 min at room temperature, followed by washing with PBS. The nuclei were stained using 4',6-diamidino-2-phenylindole (DAPI) for 15 min at room temperature, and covered using glass coverslips. The immunofluorescent stained cells

were viewed and images captured using confocal laser scanning microscopy (LSM 880NL0; Carl Zeiss). The OPG concentration was used according to the study by Zhao *et al* (5). The method used for immunofluorescence staining was as described in the study by Fathi *et al* (16).

**Scanning electron microscopy (SEM).** After the cells were treated with OPG (80 ng/ml) for 12 h, various reagents (U0126, 5  $\mu$ M; SP600125, 10  $\mu$ M; SB202190, 5  $\mu$ M) for 30 min, the cells were fixed in 2.5% glutaraldehyde solution overnight at 4°C, dehydrated using increasing concentrations of ethanol from 50-100%, dried and gold-coated (as the sample does not conduct electricity), using the carbon coater for gold coating (MC1000; Hitachi, Ltd.). Cell morphologies were observed using a Hitachi S-4800 Field-Emission Environmental Scanning Electron Microscope (Hitachi Corporation). The SEM method was as previously described in the study by Ma *et al* (14).

**Statistical analysis.** Each experiment was repeated at least three times and no data were excluded. All data were analyzed using SPSS 22.0 software (SPSS, Inc.). The results are expressed as the mean  $\pm$  standard deviation. An independent samples t-test (Student's t-test) was used for two-sample comparisons for data demonstrating a normal distribution. The t-test used was unpaired in the present study. Multiple groups were compared using one-way analysis of variance (ANOVA) followed by Tukey's or Tamhane's test.  $P < 0.05$  was considered to indicate statistically significant differences.

## Results

**OPG suppresses osteoclast adhesion-related protein expression.** The levels of osteoclast adhesion-related proteins were examined using western blot analysis. In response to OPG stimulation, the levels of osteoclast adhesion proteins, including integrin  $\alpha$ v, integrin  $\beta$ 3, p-vinculin, p-paxillin and p-SRC (527), were significantly decreased in a concentration-dependent manner (Fig. 1). However, the phosphorylation of SRC at amino acid 416 was increased following treatment with OPG, in a concentration-dependent manner (Fig. 1). Taken together, these data demonstrated that OPG inhibited the expression of osteoclast adhesion-related proteins.

**OPG damages osteoclast adhesive structures via the MAPK signaling pathways.** Firstly, MAPK signaling pathways were examined using western blot analysis. The data demonstrated OPG reduced the phosphorylation of ERK, JNK and p38 in a concentration-dependent manner, and the phosphorylation of ERK, JNK and p38 also significantly decreased at different time points by OPG treatment (Fig. 2A). These results suggested that OPG inhibited the MAPK signaling pathways.

Subsequently, specific inhibitors of ERK (U0126), JNK (SP600125) and p38 (SB202190) were used. As shown in Fig. 2B, the decrease in the levels of osteoclast adhesion proteins was significantly reversed when the cells were co-treated with OPG and U0126. The results revealed that when osteoclasts were co-treated with OPG (80 ng/ml) and U0126 (5  $\mu$ M), the levels of key osteoclast adhesion proteins

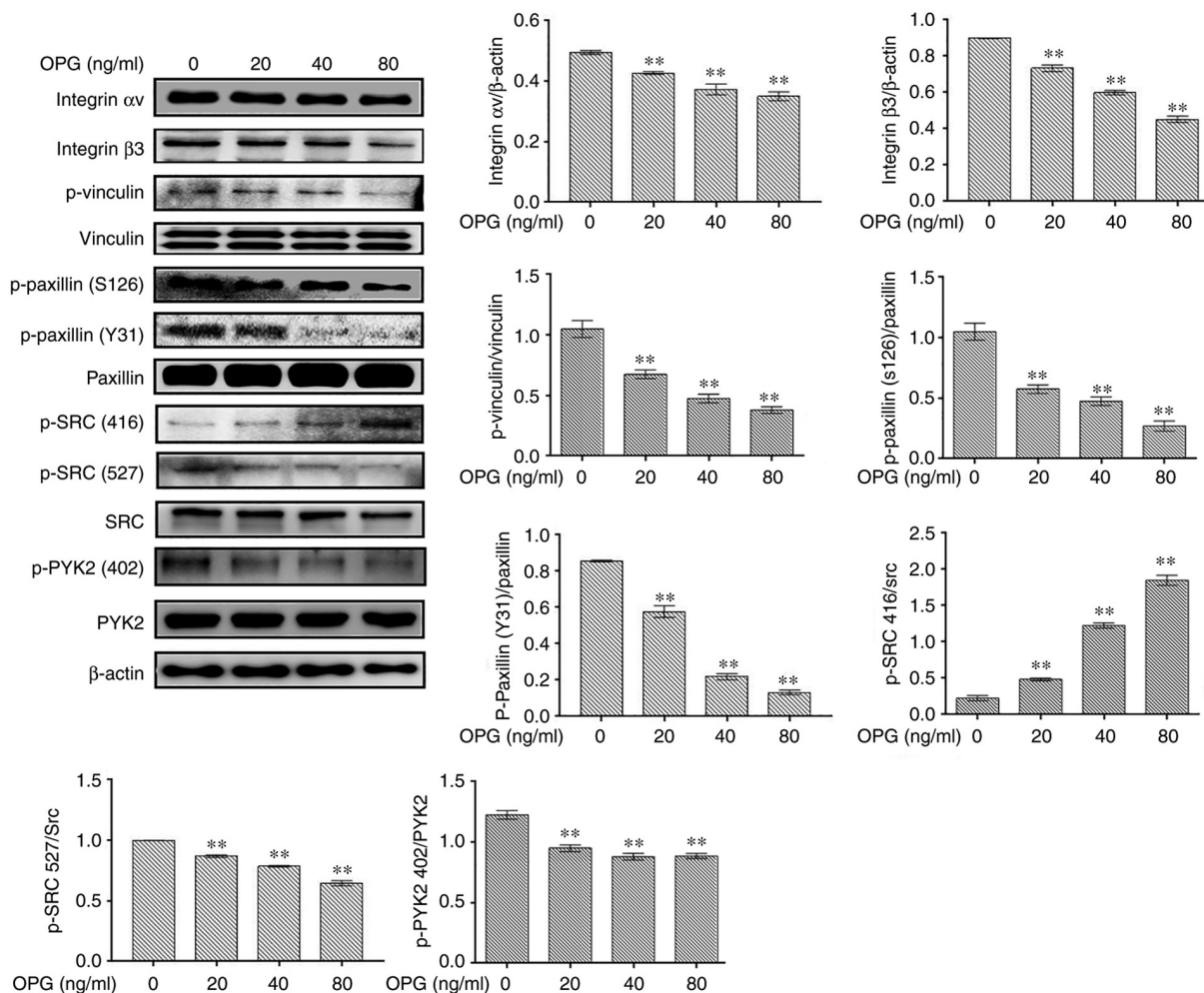


Figure 1. OPG suppresses RANKL-induced specific osteoclast adhesion protein expression. mouse bone marrow-derived macrophages were treated with macrophage colony-stimulating factor and RANKL for 5 days, followed by treatment with the indicated concentrations of OPG for 12 h. Osteoclasts were lysed and total proteins were obtained. The expression levels of osteoclast adhesion-related proteins were determined using western blot analysis. \*\**P* < 0.01 vs. controls. Data are representative of three independent experiments. OPG, osteoprotegerin; RANKL, receptor activator of the nuclear factor- $\kappa$ B (NF- $\kappa$ B) ligand; PYK2, phosphorylated protein tyrosine kinase 2; SRC, SRC proto-oncogene, non-receptor tyrosine kinase.

were higher than those in the OPG group, and the phosphorylation levels of vinculin and paxillin were mostly recovered compared with those in the OPG group. In addition, the data also revealed that OPG altered the phosphorylation levels of SRC at 416 and 527; however, no recovery of the SRC phosphorylation levels was observed in the group co-treated with OPG and U0126. Using the same method, the osteoclasts were cotreated with OPG, SP600125 (10  $\mu$ M) and SB202190 (5  $\mu$ M), respectively. As shown in Fig. 2C and D, co-treatment with OPG and the inhibitors markedly increased the levels of osteoclast adhesion-related proteins, which was consistent with the results obtained with U0126.

Subsequently, the distribution of adhesion-related proteins was analyzed using immunofluorescence staining, including integrin  $\alpha$ v, integrin  $\beta$ 3, vinculin, paxillin, SRC and PYK2. As shown in Fig. 2E, the distribution of integrin  $\alpha$ v and integrin  $\beta$ 3 and F-actin was very similar, being co-localized in the periphery of the osteoclasts. This co-localization was not observed in the OPG-treated group. OPG completely disrupted the distribution of integrin  $\alpha$ v and integrin  $\beta$ 3 to the osteoclast periphery. The labeling of integrin was diffuse inside the osteoclasts or even disappeared. Of note, the co-treatment

group exhibited a markedly altered integrin  $\alpha$ v and integrin  $\beta$ 3 location, with co-localization being observed at the osteoclast periphery. For other adhesion proteins (Fig. S1), including vinculin and paxillin, the distribution was consistent compared with that of integrin. However, SRC and PYK2 remained localized in the cell center or exhibited a diffuse distribution after treatment with OPG and inhibitors, which was consistent with the results of western blot analysis.

Finally, SEM was used to analyze the morphological changes of the adhesion structures in osteoclasts. The adhesion structure was distributed as a circular zone near the periphery of the osteoclast and outside this peripheral circular zone, including the lamellipodia and filopodia. Following treatment with OPG, as shown in Fig. 2F, a severe retraction and reduction of lamellipodia and filopodia-like structures was observed, some of which were detached from the substrate. Moreover, the osteoclast adhesion structures in the control and inhibitor groups exhibited no obvious changes. The OPG and inhibitor co-treatment groups exhibited no marked retraction and reduction in osteoclast lamellipodia and filopodia, which remained attached to the substrate. The aforementioned results indicated that MAPK was involved in regulating osteoclast adhesion structures.



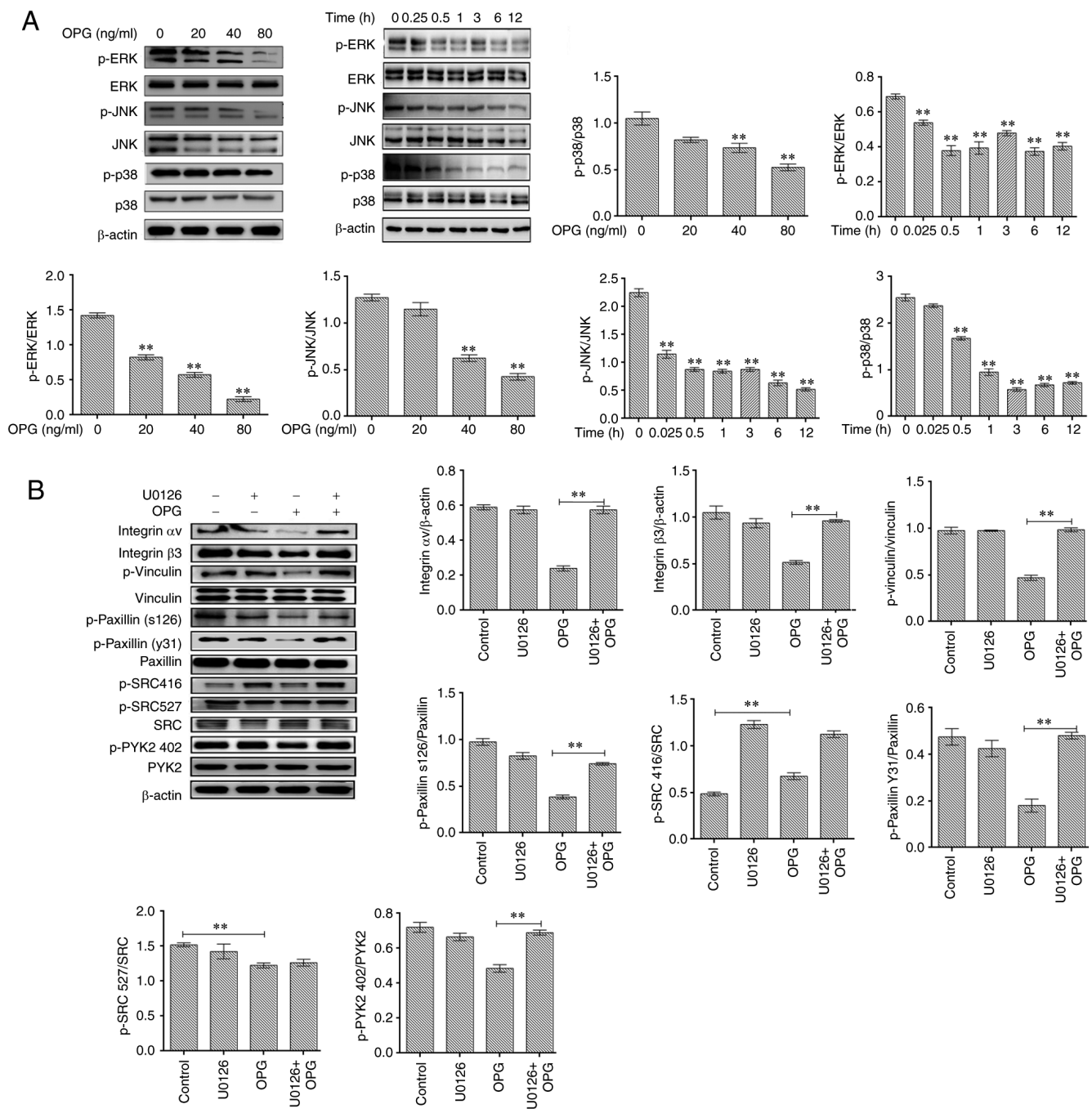
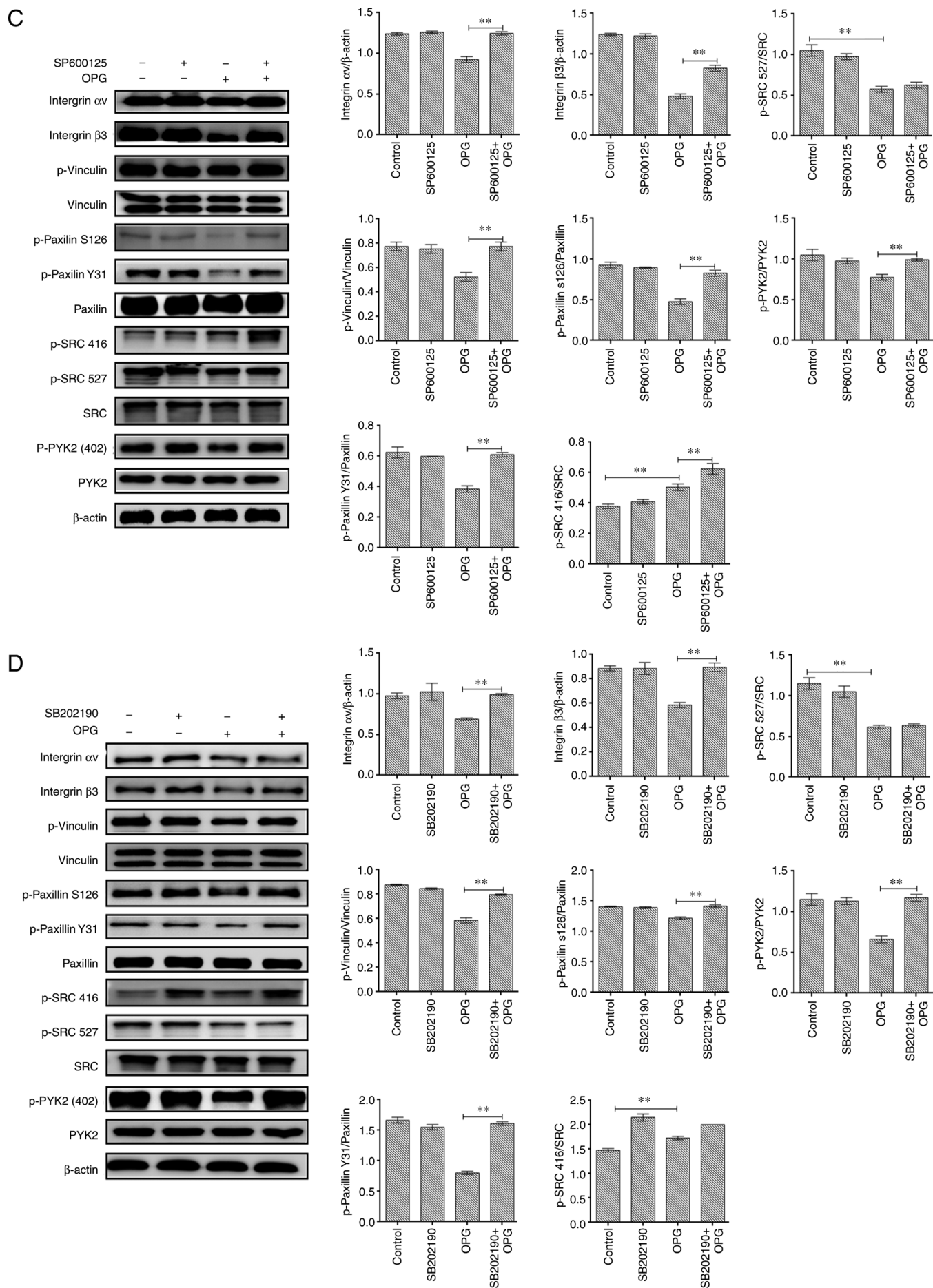


Figure 2 Continued.

**Absence of P2X7R inhibits osteoclast differentiation.** P2X7R expression was analyzed during osteoclast differentiation. The P2X7R levels were upregulated over time (1-5 days) during osteoclastogenesis (Fig. 3A). Subsequently, mouse BMMs were transfected with an adenovirus-mediated P2X7R-shRNA, and control and blank interference adenoviruses, and then cultured in the presence of RANKL (60 ng/ml) and M-CSF (30 ng/ml). The silencing efficacy of P2X7R was determined using western blot analysis (Fig. 3B). The results revealed that P2X7R deficiency suppressed the formation of TRAP-positive multinucleated osteoclasts compared with the control and blank interference adenovirus (Fig. 3C). To further illustrate the effect of P2X7R, the BMMs were treated with the P2X7R inhibitor, A438079, which does not affect cell proliferation.

After 5 days, A438079 (50  $\mu$ M/l) significantly inhibited the formation of multinucleated osteoclasts (Fig. 3D). These results suggested that P2X7R plays a crucial role in osteoclast differentiation.

**Effect of MAPK signaling inhibitors on P2X7R expression.** In the present study, osteoclasts treated with OPG (80 ng/ml) for 12 h were examined for P2X7R expression levels. The results revealed that OPG reduced the expression of P2X7R in a concentration-dependent manner, and the expression of P2X7R also significantly decreased at different time points by OPG treatment (Fig. 4A). To further illustrate that the OPG-induced reduction in P2X7R levels was related to MAPK signaling, specific inhibitors of ERK (U0126), JNK (SP600125) and





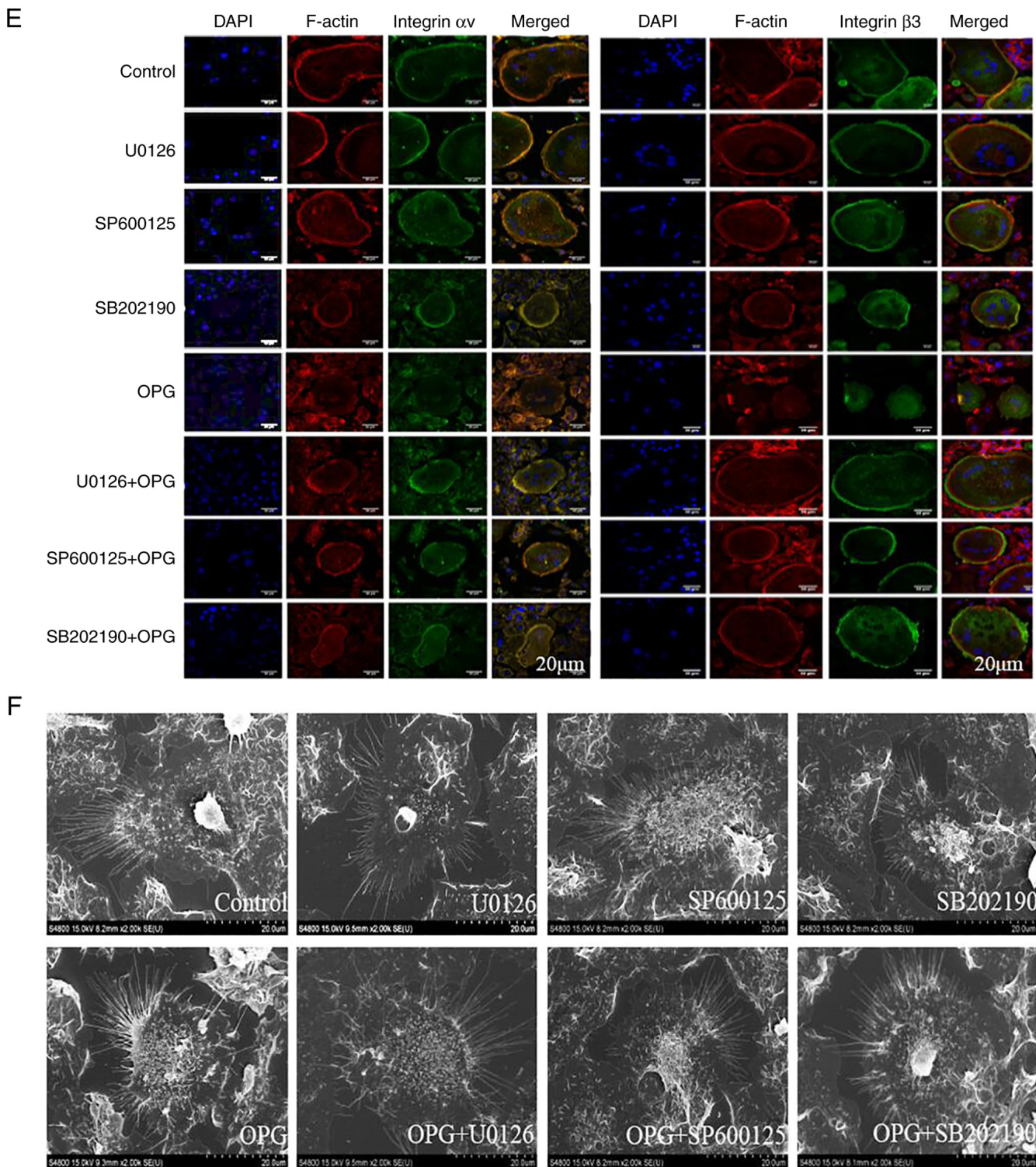


Figure 2. OPG damages osteoclast adhesive structures via the MAPK signaling pathway. Osteoclasts were differentiated from mouse bone marrow-derived macrophages in 24-well culture plates, and then cultured in  $\alpha$ -MEM in the presence of receptor activator of the nuclear factor- $\kappa$ B (NF- $\kappa$ B) ligand and macrophage colony-stimulating factor for 5 days. (A) The activation of MAPK signaling was determined using western blot analysis. \*\* $P < 0.01$ . (B-D) Effects of U0126, SB202190 and SP600125 on OPG-mediated osteoclast adhesion structures. Osteoclasts were pre-treated with 5  $\mu$ M U0126, 10  $\mu$ M SP600125 or 5  $\mu$ M SB202190 for 30 min followed by 80 ng/ml OPG for a further 12 h. Western blot analysis was performed for osteoclast adhesion-related proteins in osteoclasts exposed to OPG, or OPG and inhibitors. \*\* $P < 0.01$ . (E and F) Osteoclasts were fixed, permeabilized and stained for integrin  $\alpha v$  and  $\beta 3$ , actin and nuclei. (E) Colocalization of integrin  $\alpha v$  and  $\beta 3$  was analyzed using a confocal fluorescence microscope. Scale bars, 20  $\mu m$ . (F) Osteoclast adhesion structures were examined using scanning electron microscopy. Scale bars, 100  $\mu m$ . Data are representative of three independent experiments. OPG, osteoprotegerin; PYK2, phosphorylated protein tyrosine kinase 2; SRC, SRC proto-oncogene, non-receptor tyrosine kinase

p38 (SB202190) were used and P2X7R expression was examined. The results revealed that the OPG-induced reduction in

P2X7R levels was partially or absolutely reversed using the specific inhibitors (Fig. 4B).

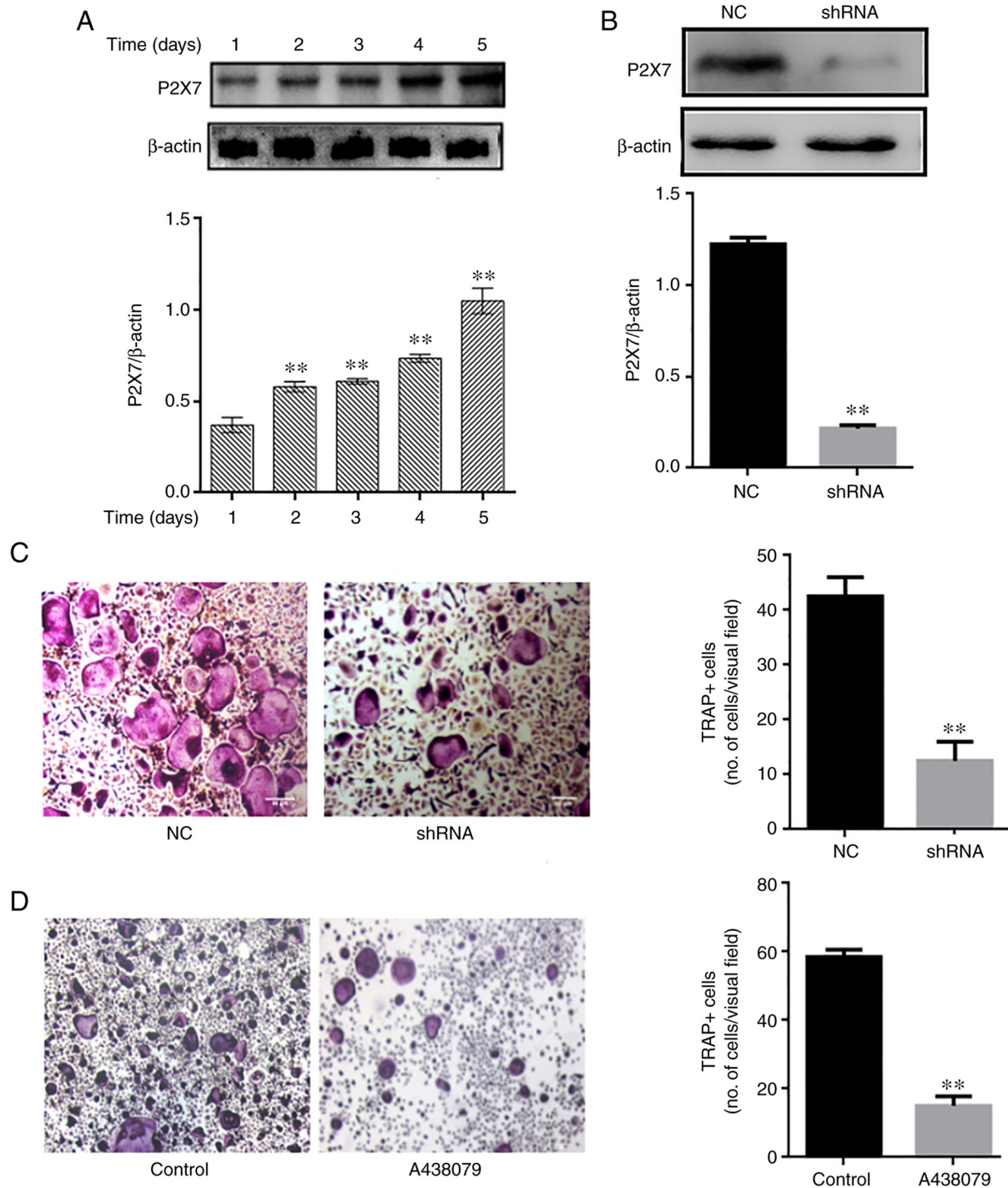


Figure 3. Absence of P2X7 inhibits osteoclast differentiation. (A) Mouse bone marrow-derived macrophages were differentiated in the presence of macrophage colony-stimulating factor and receptor activator of the nuclear factor- $\kappa$ B (NF- $\kappa$ B) ligand for 1, 2, 3, 4 and 5 days. The expression of P2X7R was examined using western blot analysis.  $^{**}P < 0.01$  vs. control. (B and C) Cells were transfected with negative control-shRNA and P2X7R-shRNA for 48 h, and the expression of P2X7R was then examined using western blot analysis and staining with TRAP (magnification,  $\times 50$ ).  $^{**}P < 0.01$ . (D) Cells were treated with A438079 (P2X7 inhibitor) for 12 h. After 5 days, TRAP staining was performed to analyze osteoclast numbers.  $^{**}P < 0.01$ . Data are representative of three independent experiments. PYK2, phosphorylated protein tyrosine kinase 2; TRAP, tartrate-resistant acidic phosphatase.

*Effect of BzATP/P2X7R-shRNA on OPG-induced osteoclast adhesion function and MAPK signaling.* Osteoclasts were treated with BzATP for 30 min, followed by OPG treatment for 12 h. In addition, the BMMs were transfected with adenovirus with P2X7R-shRNA in the presence of M-CSF and RANKL. As shown in Fig. 5A, compared with the control group, the levels of p-p38 and p-ERK, but not those of p-JNK, increased

significantly following treatment with BzATP. P2X7R-shRNA decreased the phosphorylation levels of ERK, JNK and p38 MAPK compared with those in the negative control group. The results also revealed that OPG markedly decreased the phosphorylation levels of ERK, JNK and p38. However, this phenomenon was reversed or aggravated by BzATP or P2X7R-shRNA, respectively. Therefore, these results indicated that



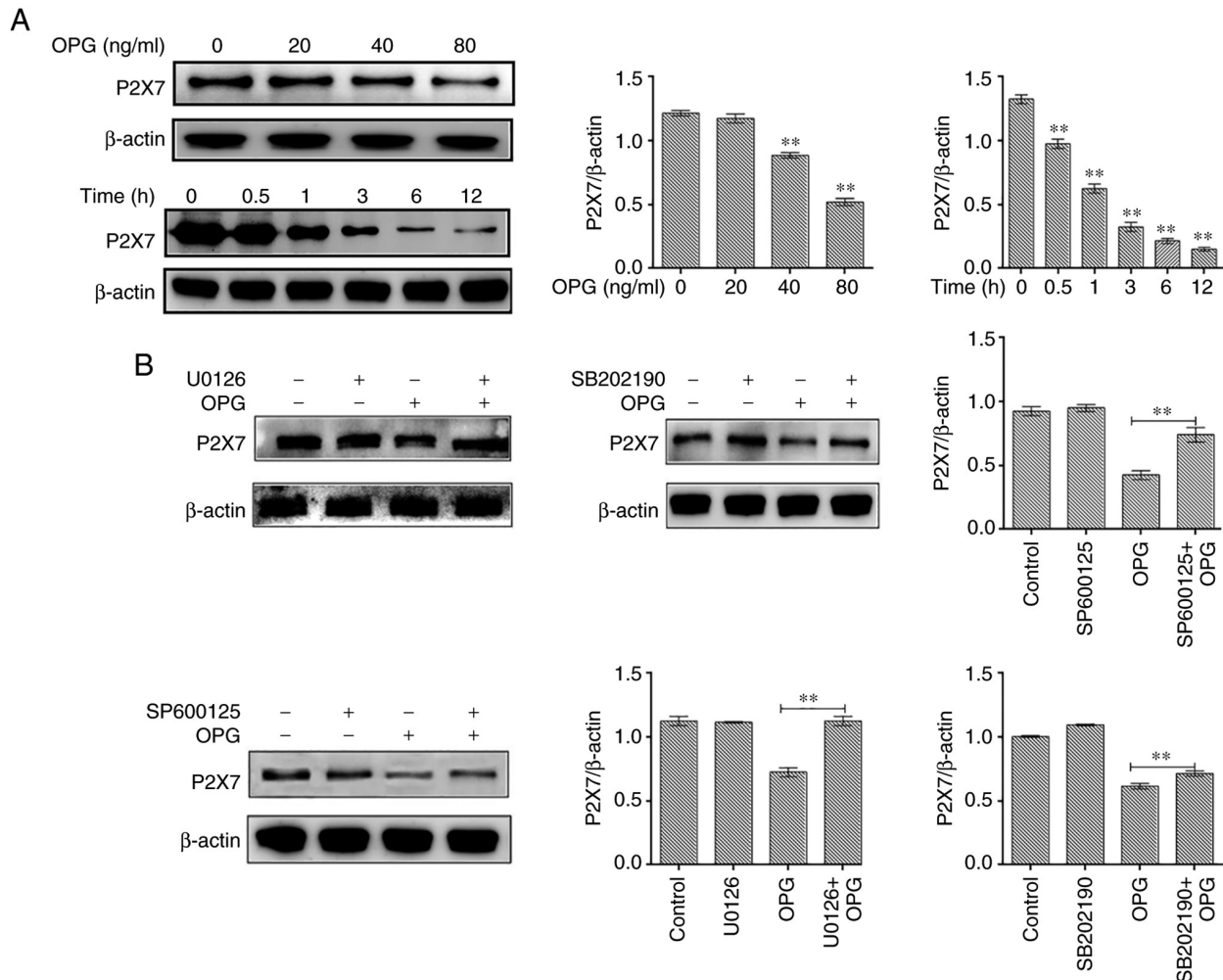


Figure 4. Effect of MAPK signaling inhibitors on P2X7 expression. (A) Mouse bone marrow-derived macrophages were cultured in the presence of macrophage colony-stimulating factor and receptor activator of the nuclear factor- $\kappa$ B (NF- $\kappa$ B) ligand for 5 days, followed by treatment with OPG (0, 20, 40 and 80 ng/ml) for a further 12 h, and treatment with OPG (80 ng/ml) for different time periods (0, 0.5, 1, 3, 6, 12 h). The expression of P2X7R was examined using western blot analysis. \*\* $P < 0.01$ . (B) Osteoclasts were pre-treated with U0126, SB202190 and SP600125 for 30 min followed by 80 ng/ml OPG for a further 12 h. The expression of P2X7R was examined using western blot analysis. \*\* $P < 0.01$  vs. control or as indicated by the lines on the graphs. Data are representative of three independent experiments. OPG, osteoprotegerin; PYK2, phosphorylated protein tyrosine kinase 2.

BzATP induced the activation of P2X7R, which activated ERK and p38. By contrast, the depletion of P2X7R markedly inhibited MAPK signaling activation.

Subsequently, the present study examined the effects of BzATP and P2X7R-shRNA on OPG-induced osteoclast adhesion function. First, western blot analysis was used to assess the levels of adhesion-related protein following treatment with BzATP, P2X7R-shRNA and OPG. As shown in Fig. 5B and C, the levels of integrin  $\alpha$ v and  $\beta$ 3 markedly decreased in the OPG group. BzATP and OPG co-treatment significantly increased the integrin  $\alpha$ v and  $\beta$ 3 levels; however, P2X7R-shRNA and OPG co-treatment further decreased the levels of integrin  $\alpha$ v and  $\beta$ 3 compared with those in the negative control plus OPG group. The results also revealed that OPG reduced the phosphorylation levels of vinculin and paxillin; however, the activation of P2X7R with BzATP markedly increased the phosphorylation levels of vinculin and paxillin. By contrast, the depletion of P2X7R markedly decreased the phosphorylation levels of vinculin and paxillin, further disrupting the osteoclast adhesion ability. The data also demonstrated a significant reduction in PYK2 phosphorylation at position 402

and SRC phosphorylation at position 527 under OPG treatment. BzATP and P2X7R-shRNA treatment increased and decreased, respectively, the activation of PYK2 and SRC. Of note, OPG increased the level of SRC phosphorylation at position 416; however, BzATP and OPG co-treatment did not recover the level of SRC phosphorylation at position 416; P2X7R-shRNA and OPG co-treatment also did not reverse the level of SRC phosphorylation at position 416.

As shown in Fig. 5D, OPG treatment resulted in a disrupted distribution of integrin  $\alpha$ v and  $\beta$ 3. However, the OPG-induced damage to the osteoclast adhesion structures was significantly aggravated when the cells were transfected with P2X7R-shRNA. This was confirmed by the observation that the OPG-induced disruption of integrin  $\alpha$ v and  $\beta$ 3 was markedly attenuated when the cells were pre-treated with BzATP for 30 min. In addition, the levels of other adhesion proteins, examined by immunofluorescence staining, were consistent with those of integrin  $\alpha$ v and  $\beta$ 3 (Fig. S2). Taken together, these results further suggested that P2X7R plays a crucial role in regulating the damage to osteoclast adhesion structures induced by OPG.



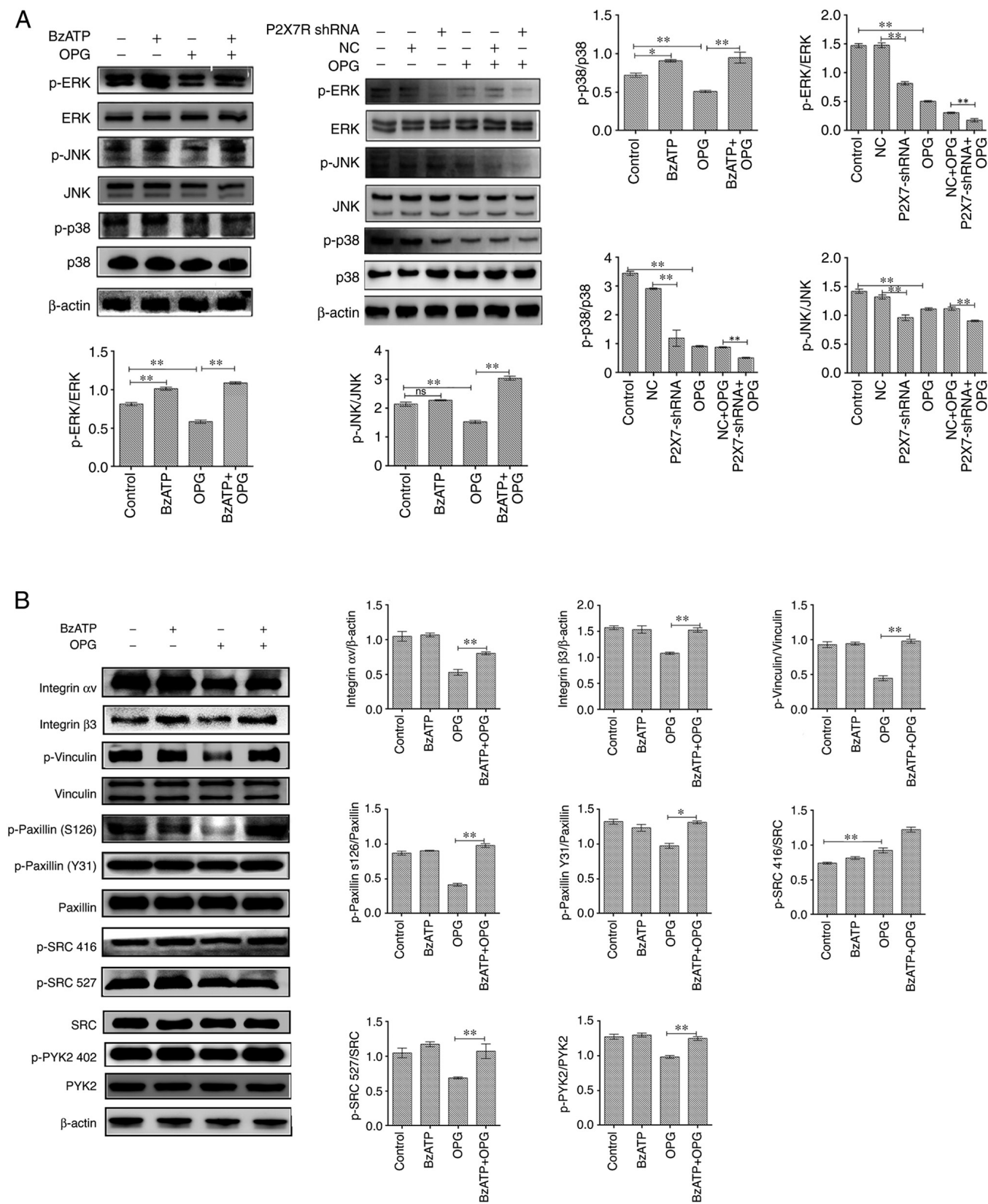
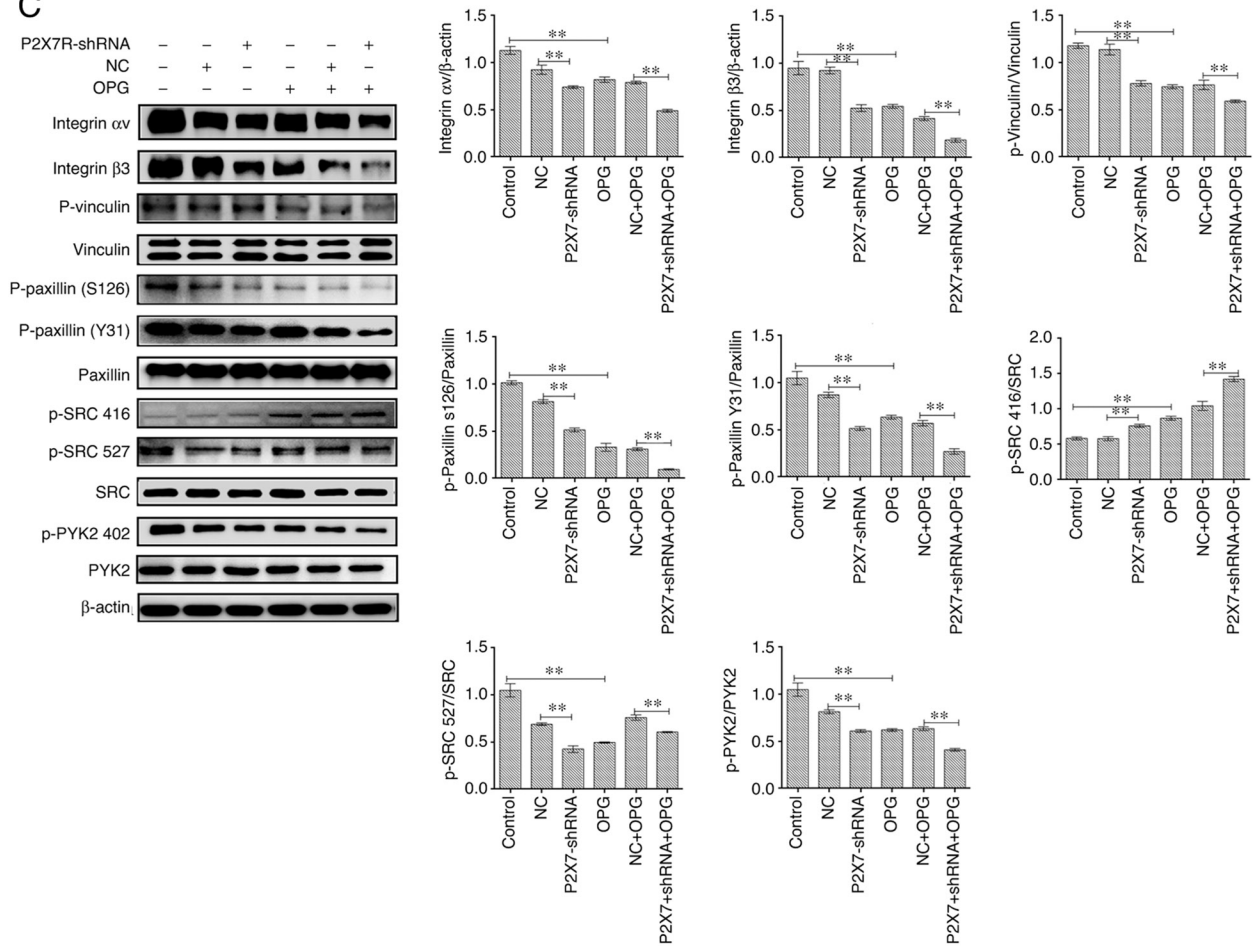


Figure 5. Continued.

SEM was then used to observe osteoclast morphology. As shown in Fig. 5E, SEM revealed that OPG severely damaged osteoclast pseudopodia, including filopodia breakage or loss of filopodia, the retraction of lamellipodia and detachment from the substrate. However, BzATP pre-treatment for 30 min

reversed these OPG-induced osteoclast morphological changes. By contrast, the depletion of P2X7R did not recover osteoclast intact morphology, but further aggravated the OPG-induced adhesive structure damage. The results of the present study thus suggest that P2X7R-mediated MAPK signaling plays an

C



D

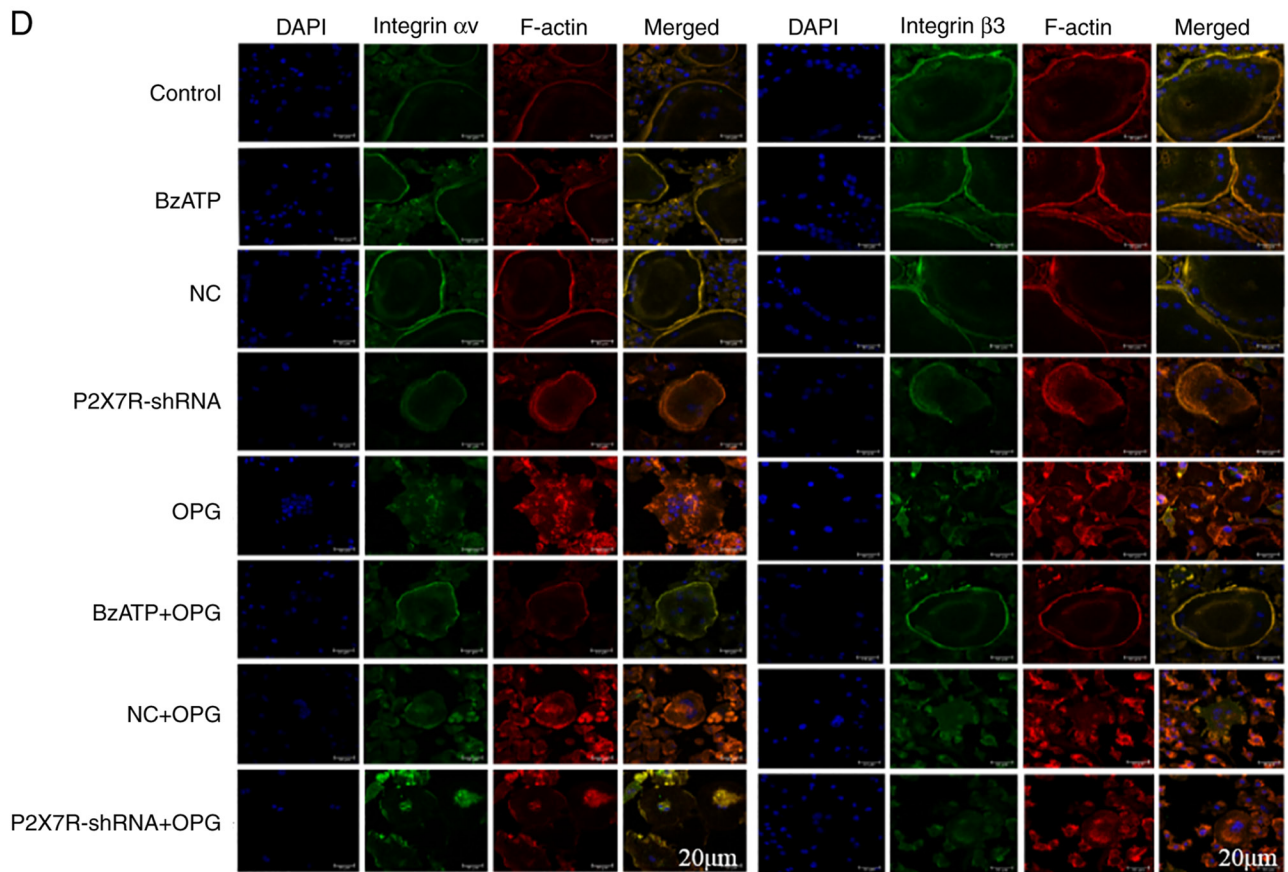


Figure 5. Continued.

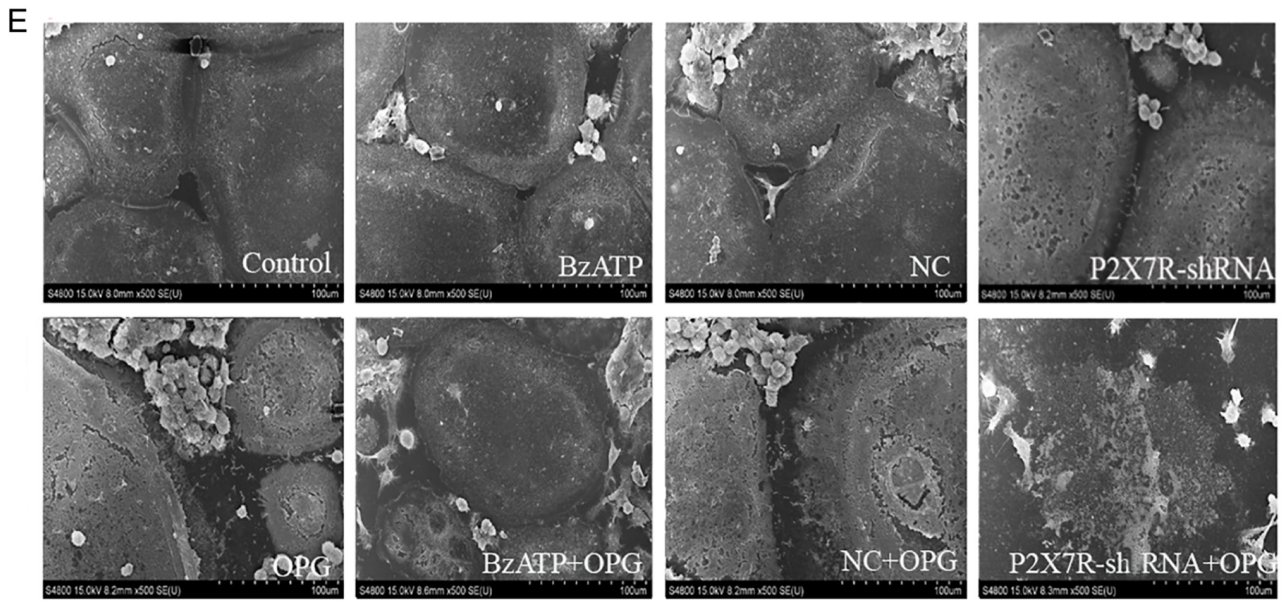


Figure 5. Effect of BzATP/P2X7R shRNA on OPG-induced osteoclast adhesion function and MAPK signaling. (A–C) Mature osteoclasts were pre-treated with 300  $\mu$ M BzATP for 30 min, followed by 80 ng/ml OPG for a further 12 h. The cells were transfected with negative control-shRNA and P2X7R-shRNA for 48 h, followed by treatment with OPG for 12 h. The activation of MAPK signaling and the levels of adhesion proteins were examined using western blot analysis. \* $P < 0.05$  and \*\* $P < 0.01$ . (D) The distribution of integrin  $\alpha$ v and  $\beta$ 3 was analyzed using a confocal fluorescence microscope. Scale bars, 20  $\mu$ m. (E) The morphology of the osteoclast adhesion structures was observed using scanning electron microscopy. Scale bars, 100  $\mu$ m. Data are representative of three independent experiments. OPG, osteoprotegerin; P2X7R, purinergic receptor P2X7; BzATP, 3'-O-(4-Benzoyl) benzoyl ATP.

essential role in resisting OPG-induced damage to osteoclast adhesion.

## Discussion

The critical role of P2X7R in bone pathogenesis has been elucidated (11). The results of the present study demonstrated that P2X7R may be a potential target for bone disease therapeutics. The results indicated that OPG disrupted osteoclast adhesive function by affecting MAPK signaling. The absence of P2X7R inhibited osteoclast function, and P2X7R-mediated-MAPK signaling was involved in OPG-induced osteoclast adhesive structure damage.

It has been previously reported that osteoclasts are multinucleated cells generated from monocytes and macrophages, which adhere to mineralized bone matrix and become polarized, forming the sealing zone for bone resorption (17). OPG has been observed to inhibit osteoclast differentiation and bone resorption by blocking the binding of RANKL to RANK (18). A previous study (19) also demonstrated that the cytoskeleton plays an important role in osteoclast differentiation, maturation and adhesion. Moreover, filopodia and podosomes undergo drastic and regular variations during osteoclast differentiation and adhesion. In the present study, OPG significantly disrupted the filopodia and lamellipodia in mature osteoclast. In addition, OPG suppressed osteoclastic adhesion protein expression, including integrin  $\alpha$ v, integrin  $\beta$ 3, p-vinculin, p-paxillin and p-SRC at position 527. SRC is an adaptor protein, and the phosphorylation of SRC at position 416 was increased by OPG. Previous research has demonstrated that podosomes and pseudopodium share several components and structural features, the most important being a multimolecular complex surrounding the core, which comprises integrin

receptors and integrin-associated proteins that are also found in focal adhesions, such as vinculin and paxillin (20). Paxillin, an adaptor protein, is highly phosphorylated on tyrosyl residues and has been shown to regulate focal adhesion dynamics and cell migration (21). In the present study, OPG significantly inhibited the phosphorylation of paxillin at tyrosine 31 (Y31) and serine (S126). Furthermore, OPG severely disrupted the distribution of paxillin in mature osteoclasts. Paxillin plays a main role in regulating osteoclast adhesion and migration. Additionally, vinculin, as an actin protein, is closely related to the maturation of podosomes (22). In the present study, OPG attenuated the phosphorylation of vinculin and disrupted its distribution. It has also been found that vinculin-deficient osteoclasts do not exhibit any actin ring formation or bone resorption activity (23). In addition, the cytokine activation of osteoclasts requires matrix-derived signals transmitted intracellularly via integrin  $\alpha$ v and  $\beta$ 3, which induces SRC to stimulate a canonical, cytoskeleton-organizing complex (24). Herein, the levels of integrin  $\alpha$ v and  $\beta$ 3 were reduced following OPG stimulation and exhibited a scattered distribution in the cell center, which would lead to osteoclasts losing their adhesion function and to the inhibition of downstream signaling. Moreover, OPG induced a decrease in PYK2 Tyr 402 and SRC Tyr 527 phosphorylation, whereas the phosphorylation of SRC at Tyr 416 was markedly increased. SRC and PYK2, as part of the podosome actin cloud, are essential for proper podosome organization and bone resorption (25). The results of the present study suggested that OPG disturbed the adhesion structure and the distribution of podosomes in osteoclasts by causing the disequilibrium of the dormant form of SRC. PYK2-null osteoclasts have been shown to be unable to form the podosome belt, resulting in impaired bone resorption (26). This finding is consistent with the findings of the present study,



in which OPG inhibited PYK2 activity, resulting in podosome disassembly and impaired osteoclast resorption ability.

M-CSF and RANKL play an essential role through MAPK signaling pathways during osteoclast differentiation and bone resorption. Of note, in the present study, OPG significantly suppressed MAPK signaling. A previous study demonstrated that OPG suppressed osteoclast differentiation by inhibiting the phosphorylation of ERK1 and ERK2, and directly induced podosome disassembly in osteoclasts (4). In the present study, the blocking of ERK signaling using U0126 significantly attenuated the damaging effects of OPG. In addition, JNK and p38 signaling also plays an important role in the regulation of apoptosis, and the formation and differentiation of osteoclasts (27,28). OPG, as an upstream signaling factor, markedly suppressed JNK and p38 activation, ultimately impairing osteoclast adhesion structures. Several inflammatory cytokines that negatively influence osteoclastogenesis via JNK and p38 inactivation have been identified, including IL-3, IL-4, IL-6 and TNF (29-31). Thus, OPG and inflammatory cytokines play similar roles in regulating JNK and p38 activity, which affects osteoclast function. In the present study, the blocking of JNK and p38 signaling protected the adhesion structure from OPG induced damage. However, ERK, JNK and p38 inhibitors did not recover SRC Tyr 416 and 527 phosphorylation under OPG induction. Thus, these findings revealed that MAPK signaling was not involved in modulating SRC activation.

P2X7R is a cation channel and can be activated by ATP (32). It has been demonstrated that P2X7R is related to diseases of the central nervous system (33), multiple sclerosis (34) and bone metabolism (35). P2X7R is expressed in osteoblasts and osteoclasts (36). In the present study, P2X7R was highly expressed in mature osteoclasts and OPG reduced the expression level of P2X7R. Previous studies have also demonstrated that P2X7R-mediated signaling drives osteoclastic fusion (37) and negatively regulates bone mineralization (38). In the present study, the depletion of P2X7R significantly reduced the number of osteoclasts. A previous study also demonstrated that the blockade of P2X7R inhibited osteoclast formation *in vitro* (39), which is consistent with the present findings. The present study also found that the depletion of P2X7R markedly suppressed osteoclast adhesion functions. However, a previous study (40) demonstrated that when RGC-5 cells were treated with BzATP (a P2X7R agonist), BzATP reversed the inhibitory effects of Mongolian compound medicine-Gurigumu-13 (GRGM) on cell apoptosis, oxidative stress and the phosphorylation of p38. P2X7R knockdown was shown to further enhance the inhibitory effect of GRGM on p38 (40). Of note, BzATP enhanced the phosphorylation of p38 and ERK and reversed the damaging effects of OPG on osteoclast adhesion in the present study. In addition, P2X7R silencing significantly inhibited the MAPK pathway and aggravated the damaging effects of OPG. In recent years, studies have demonstrated that P2X7R activation can increase cancer cell invasiveness (41) and migration (42). The present study also revealed that P2X7R activation restored the normal osteoclast adhesion structure following OPG-induced damage, which suggested that P2X7R activation would recover adhesion, invasiveness and migration functions. The silencing of P2X7R further promoted the

OPG-induced damage to the adhesion structure. In brief, P2X7R-mediated MAPK signaling plays an essential role in regulating osteoclast adhesion function, and P2X7R may be a novel target for bone disease treatment. Furthermore, mesenchymal stem cell therapy may also be promising in the treatment of a number of diseases (43). In addition, P2X7R, as a targeted therapeutic strategy, may be worthy of further exploration compared with targeted therapeutics for the treatment of acute myeloid leukemia (44).

In conclusion, the present study demonstrated that OPG disrupted the osteoclast adhesion structure via P2X7R-mediated MAPK signaling and revealed the role of P2X7R in mature osteoclasts. The findings presented herein provide a novel therapeutic target for bone diseases, such as osteoporosis.

### Acknowledgements

Not applicable.

### Funding

The present study was supported by grants from the National Nature Science Foundation of China (nos. 31702304, 31872534 and 31502128), the Natural Science Foundation of Jiangsu Province (no. BK20150447), the Natural Science Foundation Research Grants of Jiangsu Province (no. BK20181452), the China Postdoctoral Science Foundation (no. 2017M611932), the Priority Academic Program Development of Jiangsu Higher Education Institutions (PAPD) and the Graduate Innovation Project of Jiangsu Province.

### Availability of data and materials

The datasets used and/or analyzed during the current study are available from the corresponding author on reasonable request.

### Authors' contributions

ZL and HZh designed the study. YM and XS performed the cell transduction and culture. YM, RS and JZ performed the western blotting and immunofluorescence. YM, XS and HZh analyzed the data. YM and XS wrote the manuscript. ZL and JZ proofread the manuscript and confirm the authenticity of all the raw data. All authors contributed to the article, and read and approved the final manuscript.

### Ethics approval and consent to participate

The animal experimental procedures were approved by the Ethics Committee of Yangzhou University [SYXK (Su) 2017-0044].

### Patient consent for publication

Not applicable.

### Competing interests

The authors declare that they have no competing interests.

## References

- Xiong J, Piemontese M, Onal M, Campbell J, Goellner JJ, Dusevich V, Bonewald L, Manolagas SC and O'Brien CA: Osteocytes, not osteoblasts or lining cells, are the main source of the RANKL required for osteoclast formation in remodeling bone. *PLoS One* 10: e0138189, 2015.
- Lee DW, Kwon JY, Kim HK, Lee HJ, Kim ES, Kim HJ, Kim HJ and Lee HB: Propofol attenuates osteoclastogenesis by lowering RANKL/OPG ratio in mouse Osteoblasts. *Int J Med Sci* 15: 723-729, 2018.
- Theoleyre S, Wittrant Y, Couillaud S, Vusio P, Berreur M, Dunstan C, Blanchard F, Rédini F and Heymann D: Cellular activity and signaling induced by osteoprotegerin in osteoclasts: involvement of receptor activator of nuclear factor kappaB ligand and MAPK. *Biochim Biophys Acta* 1644: 1-7, 2004.
- Zhao H, Gu J, Dai N, Gao Q, Wang D, Song R, Liu W, Yuan Y, Bian J, Liu X and Liu Z: Osteoprotegerin exposure at different stages of osteoclastogenesis differentially affects osteoclast formation and function. *Cytotechnology* 68: 1325-1335, 2016.
- Zhao H, Liu X, Zou H, Dai N, Yao L, Zhang X, Gao Q, Liu W, Gu J, Yuan Y, *et al*: Osteoprotegerin disrupts peripheral adhesive structures of osteoclasts by modulating Pyk2 and Src activities. *Cell Adh Migr* 10: 299-309, 2016.
- Oshiro T, Shiotani A, Shibasaki Y and Sasaki T: Osteoclast induction in periodontal tissue during experimental movement of incisors in osteoprotegerin-deficient mice. *Anat Rec* 266: 218-225, 2002.
- Zheng QZ: Radioligands targeting purinergic P2X7 receptor. *Bioorg Med Chem Lett* 30: 127169, 2020.
- Li LZ, Yue LH, Zhang ZM, Zhao J, Ren LM, Wang HJ and Li L: Comparison of mRNA Expression of P2X receptor subtypes in different arterial tissues of rats. *Biochem Genet* 58: 677-690, 2020.
- Miteva A, Gaydukov A and Balezina O: Interaction between calcium chelators and the activity of P2X7 receptors in mouse motor synapses. *Int J Mol Sci* 21: 2034, 2020.
- Dong Y, Chen Y, Zhang L, Tian Z and Dong S: P2X7 receptor acts as an efficient drug target in regulating bone metabolism system. *Biomed Pharmacother* 125: 110010, 2020.
- Agrawal A and Gartland A: P2X7 receptors: Role in bone cell formation and function. *J Mol Endocrinol* 54: R75-R88, 2015.
- Wang N, Agrawal A, Jørgensen NR and Gartland A: P2X7 receptor regulates osteoclast function and bone loss in a mouse model of osteoporosis. *Sci Rep* 8: 3507, 2018.
- Agrawal A, Buckley KA, Bowers K, Furber M, Gallagher JA and Gartland A: The effects of P2X7 receptor antagonists on the formation and function of human osteoclasts in vitro. *Purinergic Signal* 6: 307-315, 2010.
- Ma Y, Zhao H, Chile C, Wang C, Zheng J, Song R, Zou H, Gu J, YanYuan, Bian J and Liu Z: The effect of P2X7R-mediated Ca<sup>2+</sup> signaling in OPG-induced osteoclasts adhesive structure damage. *Experimental Cell Research* 43: 39-98, 2019.
- Fathi E, Farahzadi R and Valipour B: Alginate/gelatin encapsulation promotes NK cells differentiation potential of bone marrow resident C-kit hematopoietic stem cells. *Int J Biol Macromol* 177: 317-327, 2021.
- Fathi E, Farahzadi R, Viator I and Javanmardi S: Cardiac differentiation of bone-marrow-resident c-kit<sup>+</sup> stem cells by L-carnitine increases through secretion of VEGF, IL-6, IGF-I, and TGF- $\beta$  as clinical agents in cardiac regeneration. *J Biosci* 45: 92, 2020.
- Kwon JO, Jin WJ, Kim B, Kim HH and Lee ZH: Myristoleic acid inhibits osteoclast formation and bone resorption by suppressing the RANKL activation of Src and Pyk2. *Eur J Pharmacol* 768: 189-198, 2015.
- Tong X, Gu J, Song R, Wang D, Sun Z, Sui C, Zhang C, Liu X, Bian J and Liu Z: Osteoprotegerin inhibit osteoclast differentiation and bone resorption by enhancing autophagy via AMPK/mTOR/p70S6K signaling pathway in vitro. *J Cell Biochem*: Sep 6, 2018 (Epub ahead of print).
- Song RL, Liu XZ, Zhu JQ, Zhang JM, Gao Q, Zhao HY, Sheng AZ, Yuan Y, Gu JH, Zou H, *et al*: New roles of filopodia and podosomes in the differentiation and fusion process of osteoclasts. *Genetics Mol Res* 13: 4776-4787, 2014.
- Badowski C, Pawlak G, Grichine A, Chabadel A, Oddou C, Jurdic P, Pfaff M, Albighès-Rizo C and Block MR: Paxillin phosphorylation controls invadopodia/podosomes spatiotemporal organization. *Mol Biol Cell* 19: 633-645, 2008.
- Bowden ET, Barth M, Thomas D, Glazer RI and Mueller SC: An invasion-related complex of cortactin, paxillin and PKC $\mu$  associates with invadopodia at sites of extracellular matrix degradation. *Oncogene* 18: 4440-4449, 1999.
- Destaing O, Saltel F, Gémard JC, Jurdic P and Bard F: Podosomes display actin turnover and dynamic self-organization in osteoclasts expressing actin-green fluorescent protein. *Mol Biol Cell* 14: 407-416, 2003.
- Fukunaga T, Zou W, Warren JT and Teitelbaum SL: Vinculin regulates osteoclast function. *J Biological Chemistry* 289: 13554-13564, 2014.
- Zou W, Kitaura H, Reeve J, Long F, Tybulewicz VL, Shattil SJ, Ginsberg MH, Ross FP and Teitelbaum SL: Syk, c-Src, the  $\alpha$ v $\beta$ 3 integrin, and ITAM immunoreceptors, in concert, regulate osteoclastic bone resorption. *J Cell Biol* 176: 877-888, 2007.
- Novack DV and Faccio R: Osteoclast motility: Putting the brakes on bone resorption. *Ageing Res Rev* 10: 54-61, 2011.
- Buckbinder L, Crawford DT, Qi H, Ke HZ, Olson LM, Long KR, Bonnette PC, Baumann AP, Hambor JE, Grasser WA III, *et al*: Proline-rich tyrosine kinase 2 regulates osteoprogenitor cells and bone formation, and offers an anabolic treatment approach for osteoporosis. *Proc Natl Acad Sci USA* 104: 10619-10624, 2007.
- Otero JE, Dai S, Foglia D, Alhawagri M, Vacher J, Pasparakis M and Abu-Amer Y: Defective osteoclastogenesis by IKK $\beta$ -null precursors is a result of receptor activator of NF- $\kappa$ B ligand (RANKL)-induced JNK-dependent apoptosis and impaired differentiation. *J Biol Chem* 283: 24546-24553, 2008.
- Lacey DL, Timms E, Tan HL, Kelley MJ, Dunstan CR, Burgess T, Elliott R, Colombero A, Elliott G, Scully S, *et al*: Osteoprotegerin ligand is a cytokine that regulates osteoclast differentiation and activation. *Cell* 93: 165-176, 1998.
- Khapli SM, Tomar GB, Barhanpurkar AP, Gupta N, Yogesha SD, Pote ST and Wani MR: Irreversible inhibition of RANK expression as a possible mechanism for IL-3 inhibition of RANKL-induced osteoclastogenesis. *Biochem Biophys Res Commun* 399: 688-693, 2010.
- Yoshitake F, Itoh S, Narita H, Ishihara K and Ebisu S: Interleukin-6 directly inhibits osteoclast differentiation by suppressing receptor activator of NF- $\kappa$ B signaling pathways. *J Biol Chem* 283: 11535-11540, 2008.
- Takayanagi H, Ogasawara K, Hida S, Chiba T, Murata S, Sato K, Takaoka A, Yokochi T, Oda H, Tanaka K, *et al*: T-cell-mediated regulation of osteoclastogenesis by signalling cross-talk between RANKL and IFN- $\gamma$ . *Nature* 408: 600-605, 2000.
- Greenberg S, Di Virgilio F, Steinberg TH and Silverstein SC: Extracellular nucleotides mediate Ca<sup>2+</sup> fluxes in J774 macrophages by two distinct mechanisms. *J Biol Chem* 263: 10337-10343, 1988.
- McLarnon JG, Ryu JK, Walker DG and Choi HB: Upregulated expression of purinergic P2X(7) receptor in Alzheimer disease and amyloid-beta peptide-treated microglia and in peptide-injected rat hippocampus. *J Neuropathol Exp Neurol* 65: 1090-1097, 2006.
- Yiangou Y, Facer P, Durrenberger P, Chessell IP, Naylor A, Bountra C, Banati RR and Anand P: COX-2, CB2 and P2X7-immunoreactivities are increased in activated microglial cells/multiple sclerosis and amyotrophic lateral sclerosis spinal cord. *BMC Neurol* 6: 12, 2006.
- Jørgensen N: The purinergic P2X7 ion channel receptor a 'repair' receptor in bone. *Curr Opin Immunol* 52: 32-38, 2018.
- Wesselius M, Bours M, Agrawal A, Gartland A, Dagnelie P, Schwarz P and Jørgensen N: Role of purinergic receptor polymorphisms in human bone. *Front Biosci (Landmark Ed)* 16: 2572-2585, 2011.
- Pellegatti P, Falzoni S, Donvito G, Lemaire I and Di Virgilio F: P2X7 receptor drives osteoclast fusion by increasing the extracellular adenosine concentration. *FASEB J* 25: 1264-1274, 2011.
- Syberg S, Schwarz P, Petersen S, Steinberg T, Jensen JE, Teilmann J and Jørgensen NR: Association between P2X7 receptor polymorphisms and bone status in mice. *J Osteoporos* 2012: 637986, 2012.
- Gartland A, Buckley KA, Hipskind RA, Perry MJ, Tobias JH, Buell G, Chessell I, Bowler WB and Gallagher JA: Multinucleated osteoclast formation in vivo and in vitro by P2X7 receptor-deficient mice. *Crit Rev Eukaryot Gene Expr* 13: 243-253, 2003.
- Zhang QL, Wang W, Jiang Y, A-Tuya, Dongmei, Li LL, Lu ZJ, Chang H and Zhang TZ: GRGM-13 comprising 13 plant and animal products, inhibited oxidative stress induced apoptosis in retinal ganglion cells by inhibiting P2RX7/p38 MAPK signaling pathway. *Biomed Pharmacother* 101: 494-500, 2018.



41. Jelassi B, Chantôme A, Alcaraz-Pérez F, Baroja-Mazo A, Cayuela ML, Pelegrin P, Surprenant A and Roger S: P2X(7) receptor activation enhances SK3 channels- and cystein cathepsin-dependent cancer cells invasiveness. *Oncogene* 30: 2108-2122, 2011.
42. Takai E, Tsukimoto M, Harada H and Kojima S: Autocrine signaling via release of ATP and activation of P2X7 receptor influences motile activity of human lung cancer cells. *Purinergic Signal* 10: 487-497, 2014.
43. Fathi E, Sanaat Z and Farahzadi R: Mesenchymal stem cells in acute myeloid leukemia: A focus on mechanisms involved and therapeutic concepts. *Blood Res* 54: 165-174, 2019.
44. Fathi E, Farahzadi R, Sheervalilou R, Sanaat Z and Vietor I: A general view of CD33<sup>+</sup> leukemic stem cells and CAR-T cells as interesting targets in acute myeloblastic leukemia therapy. *Blood Res* 55: 10-16, 2020.



This work is licensed under a Creative Commons Attribution-NonCommercial-NoDerivatives 4.0 International (CC BY-NC-ND 4.0) License.